PRACTICAL APPLICATIONS OF CFD IN HEAT PROCESSING

Three case histories show how computational fluid dynamics (CFD) simulations can be used to determine the effect of external fluid flow on heat transfer rates in gas quenching and gas drying of metal parts.

by Andrew L. Banka
Airflow Sciences Corp.
Livonia, Michigan

Many heat processing operations rely strongly on achieving specific heat transfer rates. An obvious example is quenching, where the desired metallurgical properties will not be developed if the heat transfer rate is wrong. Moreover, nonuniformity of heat transfer rate within a single part can lead to variations in hardness, distortion, and residual stress. Similarly, nonuniform heat transfer rates across a load in a heat treating operation can lead to variations in part quality, and longer processing times may be needed to reach target processing temperatures.

Studies of heat treating operations, however, often apply an assumed heat transfer coefficient to the part surface. In many cases, the heat transfer coefficient is assumed to be uniform on all part surfaces. For liquid quench systems, in which the heat transfer rate is governed by film boiling, this may be a reasonable assumption. In many other situations, such as gas quenching, the heat transfer rates are unlikely to be constant. The design of gas flow systems may also be suboptimal, leading to greater nonuniformity than would occur simply from the geometry of the parts and loading configuration. Since the trend in the industry is to move away from liquid processing and toward gas processing, the design of gas flow systems for materials processing applications is becoming increasingly important.

This article reviews three examples of gas flow / heat transfer situations and their analysis using computational fluid dynamics (CFD) simulations. The first involves the gas quenching of a steel bar, which shows significant variation of heat transfer rate around the periphery of the part. In the second example, an impingement heating system for parts drying is shown to benefit from the use of a modified jet pattern. The final example involves the development of a high-convection carburizing furnace. Revisions to the parts loading pattern led to improved productivity, better uniformity, and reduced cycle times.

The examples demonstrate that the geometry of the part, design of the gas delivery system, and parts loading pattern can all have an effect on the efficiency of the system, the uniformity of heat transfer rate, and the resultant part quality. CFD simulations are shown to be an effective way of evaluating the effect of gas flows in current systems and developing improvements to them.

For more information:
Andrew Banka, P.E.
Technical Director
Airflow Sciences Corp.
12190 Hubbard St.
Livonia, MI 48150-1737
tel: 734 / 525-0300
fax: 734 / 525-0303
e-mail: abanka@airflowsciences. com
Web: www.airflowsciences.com

This article is based on "Using Numerical Simulations to Determine the Effect of External Fluid Flow on Heat Transfer Rates in Heat Treating Operations," a paper presented by the author at the 22nd Heat Treating Society Conference and 2nd International Surface Engineering Congress (Sept. 15–17, 2003, Indianapolis), and published by ASM International, Materials Park, Ohio, in the event proceedings (2003, p. 125–130).

Gas Quenching of Round Bar

CASE HISTORY ONE

A 10 cm (4 in.) round bar is quenched in 20 bar (290 psi), 20 m / s (100 ft / s) air in crossflow. The initial bar temperature is 1000 K (725°C, 1340°F) and the air temperature is 300 K (25°C, 80°F). The results for the first 30 seconds of quench are presented here. Constant material properties are assumed for the steel bar, and the latent heat of phase change is not included in the analysis.

The flow field around the bar is shown in Fig. 1. The top half of the figure shows the total velocity; the lower half, the stream function. The boundaries between colors in the stream function plot are streamlines in the flow field. As can be seen, the velocity is low at the front of the cylinder due to stagnation, reaches a peak near 80° from the flow impingement point, and then separates from the cylinder surface near 120°. The velocity in the wake region is low.

Figure 2 plots the surface heat transfer coefficient as a function of angle at four times during the first 30 seconds of quench. As might be expected from the velocity field, the heat transfer coefficient starts out moderate, has a peak corresponding to the peak velocity, and drops to a low value in the wake region. Overall, there is a factor of four between the peak and minimum heat transfer rates.

The surface temperature distribution around the bar is shown in Fig. 3 for the same four times as the heat transfer coefficient (Fig. 2). Following the heat transfer curves, the surface temperature is lowest near the peak velocity point and is highest in the wake. In contrast to the heat transfer coefficients, which are relatively constant with time, the variation in surface temperature increases for the portion of the quench shown. At 5 seconds, the maximum difference is 100 K (100°C, 180°F), but increases to 150 K (150°C, 270°F) at 30 seconds.

The temperature distribution within the bar is shown for four time slices in Fig. 4. The variation in surface heat transfer rates is manifest in a shift in the peak temperature point rearward from the center of the bar. The different time-temperature histories around the bar, and the variations in the temperature gradients, may lead to variations in hardness and residual stress, which may lead to distortion.

This round bar example is, in some respects, an ideal case, in that the flow presented to it is uniform and there is no obstruction from other parts. The variation in heat transfer rate is due only to the geometry of the part itself. In real situations, variations in the inlet gas stream and obstructions from neighboring parts can increase the variation.

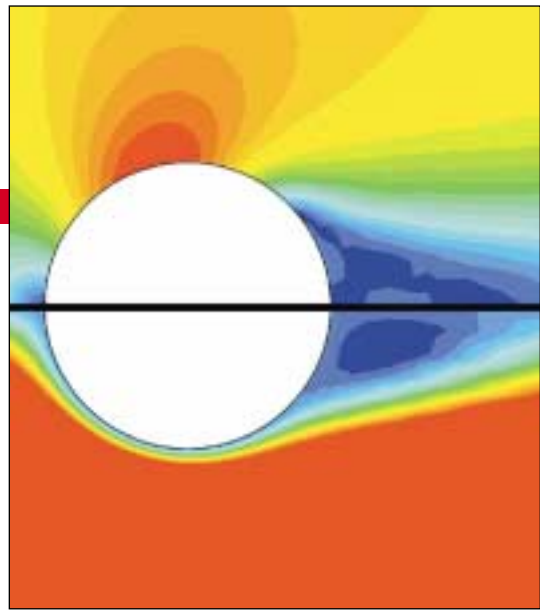

Fig. 1 — Total velocity, top, and stream function, bottom, around the cylinder.

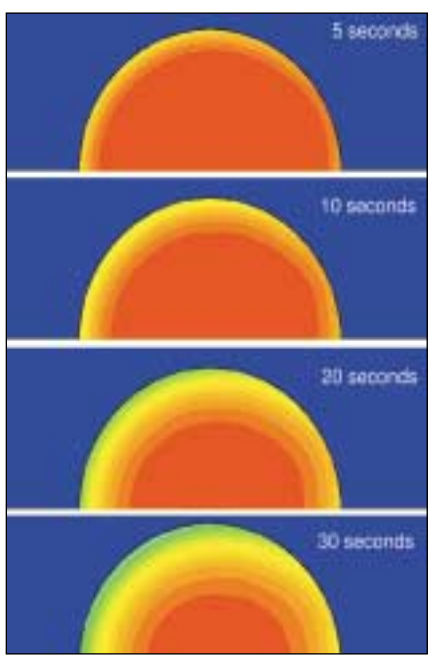

Fig. 4 — Temperature distribution within the cylinder.

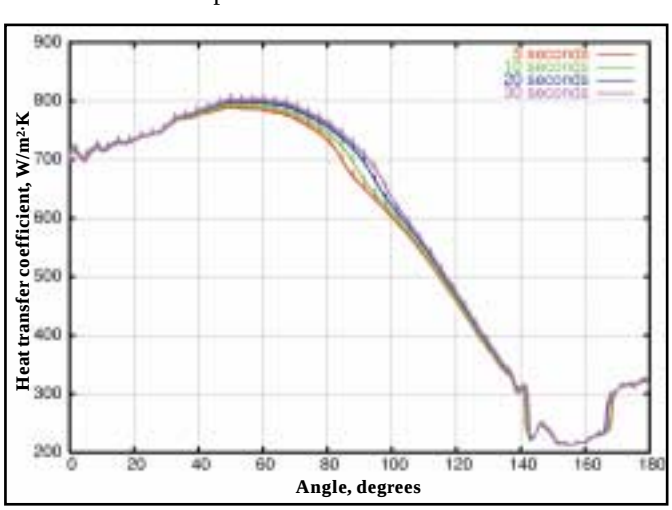

Fig. 2 — Heat transfer coefficient around the cylinder.

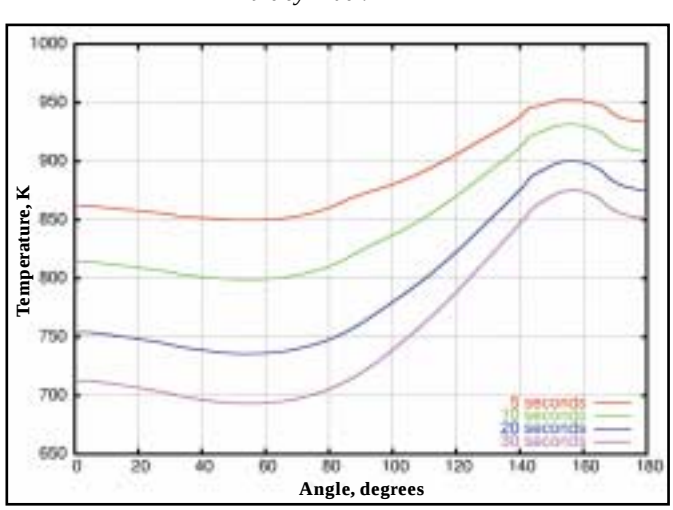

Fig. 3 — Surface temperature distribution around the cylinder.

Impingement Heating System

CASE HISTORY TWO

An impingement heating system was developed for a drying application. A pressurized plenum above the surface to be heated was used. Holes in the bottom of the plenum formed jets that would impinge on the target surface. After impingement, the flow would travel laterally to exit the device.

The initial design (Fig. 5) used a large number of relatively small holes, ostensibly to improve uniformity of heat transfer at the surface. Simulation of the flow and heat transfer, as shown in Fig. 5, indicates that the lateral flow of the exiting gases was strong enough to deflect the jets and reduce their effectiveness. Note that in this figure and in Figures 6–8, the simulation domain was limited to a single row of jets. The lateral velocity increases as the exit is approached, and so the jet deflection is strongest near the exit.

Since the lateral velocity is related to the height of the plenum above the surface (for a given flow volume), it was suspected that less jet deflection may result from a larger plenum distance. In Fig. 6, this distance has been increased from 1 in. (25 mm) to 2 in. (50 mm), but the heat transfer rate has decreased without any increase in uniformity. It would appear that the strength of the jets, for the initial hole pattern, is just too weak.

Simulated results for an alternate hole pattern at the original 1 in. (25 mm) spacing is shown in Fig. 7. Rather than a large number of small holes, a widely spaced pattern of larger holes has been used. Note that the flow volume of air has been retained, but the total area of holes has decreased, resulting in jet velocities approximately three times greater than before. These jets are unaffected by the lateral flow, and the heat transfer rates are much greater than for the original hole pattern.

A second simulation of this hole pattern was made at a distance of 5 in. (125 mm). These results, presented in Fig. 8, show that this hole pattern is also effective at larger distances. The peak heat transfer rates are reduced somewhat from the 1 in. (25 mm) results, but the uniformity of heat transfer has increased.

Article continues on p. 48

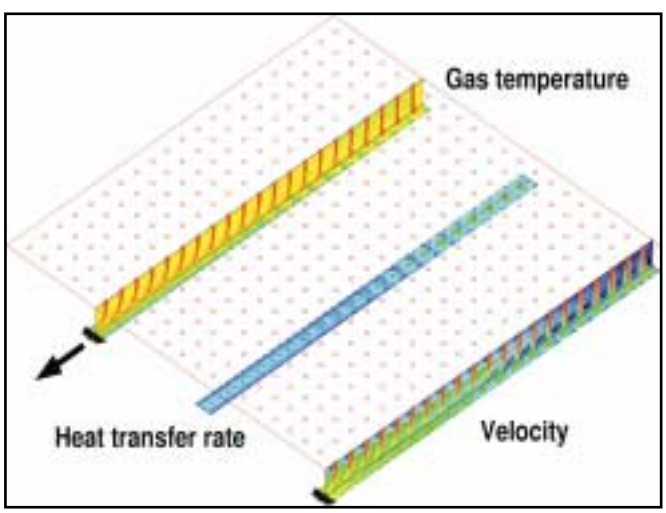

Fig. 5 — Temperature, heat transfer rate, and velocity patterns for initial hole pattern at 1 in. (25 mm) distance from the surface.

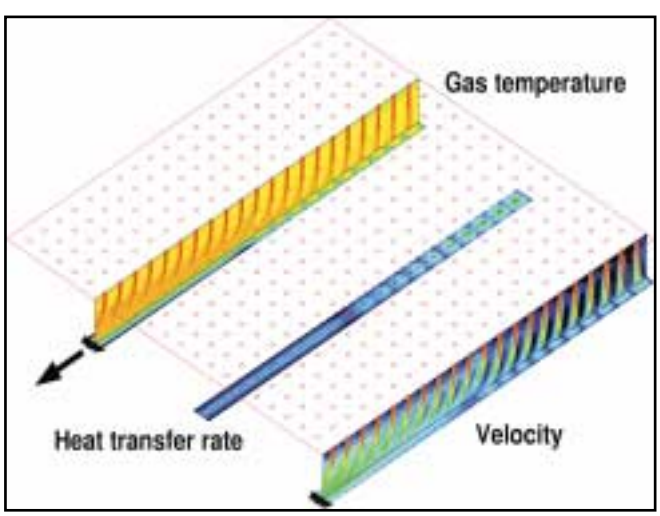

Fig. 6 — Simulated performance for initial hole pattern with 2 in. (50 mm) distance from the surface.

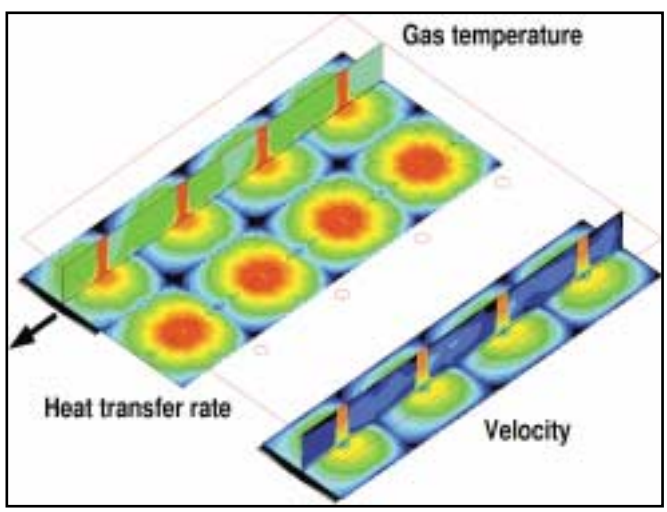

Fig. 7 — Alternate hole pattern results for 1 in. (25 mm) distance from the surface.

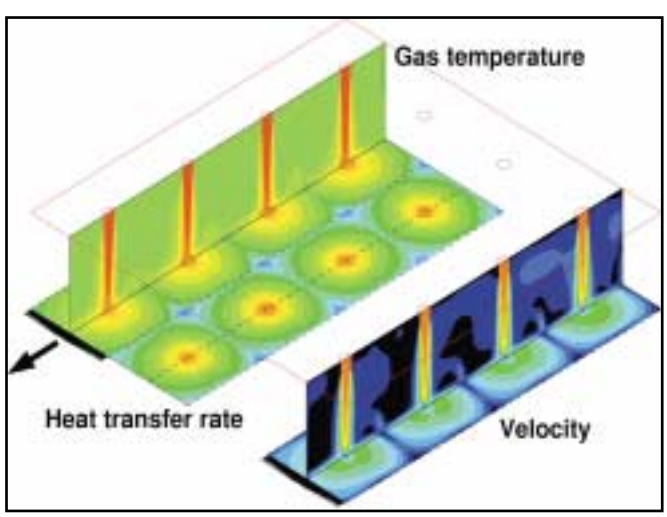

Fig. 8 — Alternate hole pattern results for 5 in. (125 mm) spacing from the surface.

High-Convection Carburizing

CASE HISTORY THREE

A novel concept for a carburizing furnace was developed with the goals of shortening cycle times and improving uniformity by providing high convective heat transfer rates to the parts. Since the gas would flow through the load of parts, the heat-up rate at internal locations would be faster and more uniform than relying on heat re-radiation from the outer portions of the load. The target load for this furnace was a dense load of pinion gears.

The overall design of the carburizing furnace is shown in Fig. 9. A separate heating chamber was used to shield the load from the high temperature of the radiant tubes. The workload section geometry was chosen to provide a relatively small cross-sectional area, thereby maximizing the gas velocity for a given gas flow volume. The workload consisted of four stacks of parts. Each stack contained a base tray and four fixtures stacked vertically. Each fixture held a single layer of 73 pinion gears.

Flow field results for this initial loading pattern are shown in Fig. 10. Due to the high flow resistance of the load, a significant portion of the circulating gases flow around the load in the gaps between the sidewalls and the ceiling. Figure 10(a) shows that the ceiling has been lowered to minimize this effect, but reasonable gaps must be maintained to account for variations and warpage in base trays and fixtures. In Fig. 10(b), the bands of higher velocity within the load correspond to the open vertical space between the top of the gears on one fixture and the bottom of the next fixture in the stack. Velocities through the load in these plots represent the bulk velocities at those locations, and not the actual velocities that would occur due to the presence of the gears and fixtures.

Flow through the workload section of the furnace can be thought of as a resistance network, in which the flow rates through the load and around the load form parallel paths. Since the resistance of the parts is much greater than the resistance of the gaps around the load, flow is biased toward the gaps until the pressure drop along these parallel paths is equal. Thus, more flow can be encouraged to flow through the load if its resistance can be reduced.

Figure 11(a) presents the flow field through a representative section of the baseline gear loading pattern. The narrow gaps between the parts create repeated acceleration and deceleration of the flow, which leads to high pressure losses. An alternate loading pattern, shown in Fig. 11(b), spaces the gears farther apart, reducing the peak velocities. As a result, the pressure loss across the load is reduced by 82% over the baseline arrangement. While this new arrangement reduces the single-layer gear count from 73 to 45, double stacking the gears on the fixture allows the loading to increase to 90 gears.

A comparison of the flow through the load for the original and revised gear loading patterns is presented in Fig. 12. The average bulk velocity through the gears has increased from 3.0 m / s (10 ft / s) for the baseline case to 5.2 m / s (17 ft / s) for the revised pattern.

Using this velocity pattern, a transient heat-up simulation was made. This simulation included convective heat transfer from the gas to the gears, fixtures, base trays, and walls. Radiation from the walls to the load and re-radiation within the load were also included. Gas participation in the radiation was included, but was not thought to be significant due to the short beam lengths involved in the furnace. The simulation predicted both gas temperatures and gear temperatures as a function of time. Separate gear temperatures were tracked for each location within the load.

The gas temperature distribution along the centerline of the furnace is shown in Fig. 13 at 10 minutes into the heating cycle. A significant gradient of gas temperature is

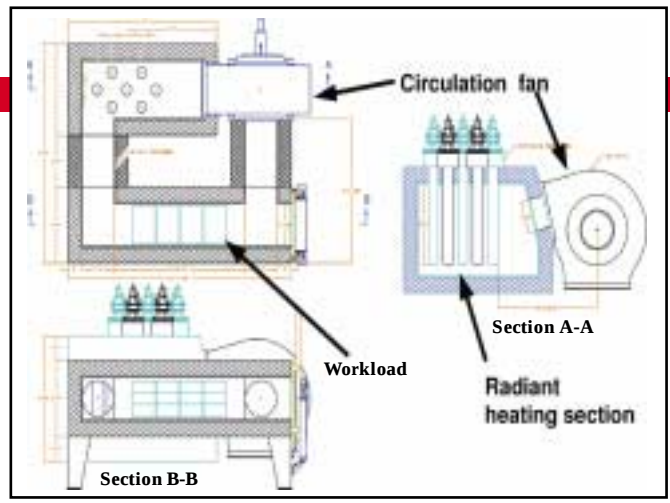

Fig. 9 — Layout of proposed high-convection carburizing furnace.

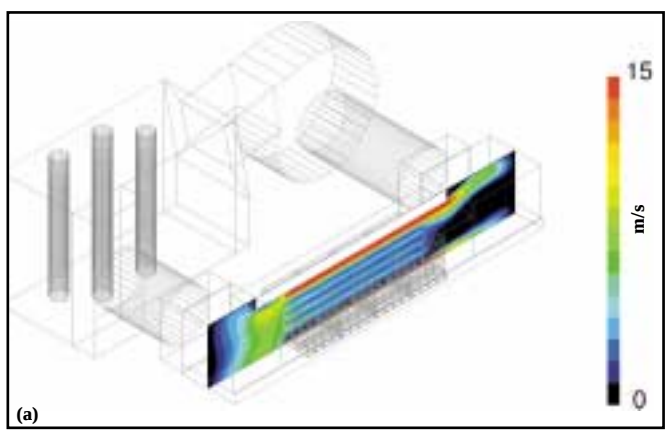

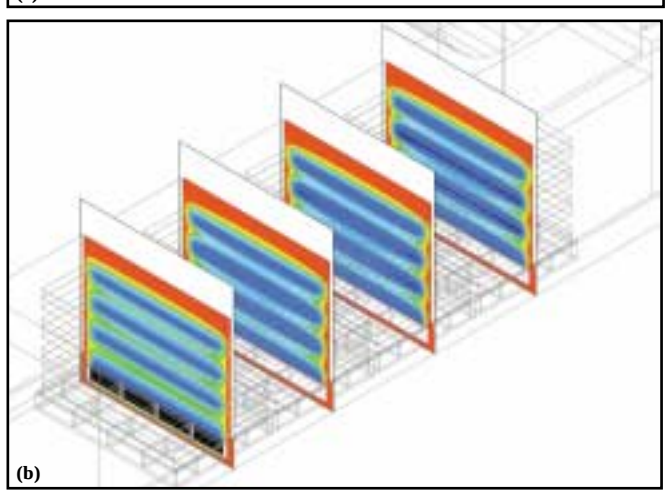

Fig. 10 — (a) Total velocity distribution along furnace centerline. (b) Lateral sections through the load showing low-velocity regions.

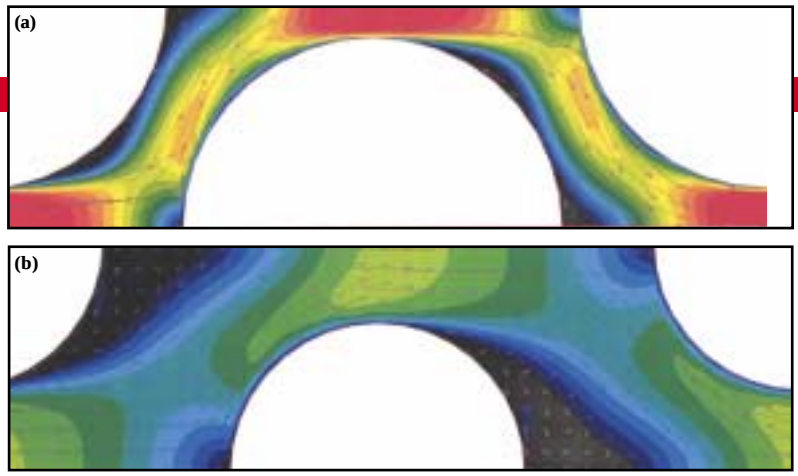

Fig. 11 — (a) Initial loading pattern, 73 gears on a single level. (b) Alternate loading pattern, 45 gears on each of two levels (90 total).

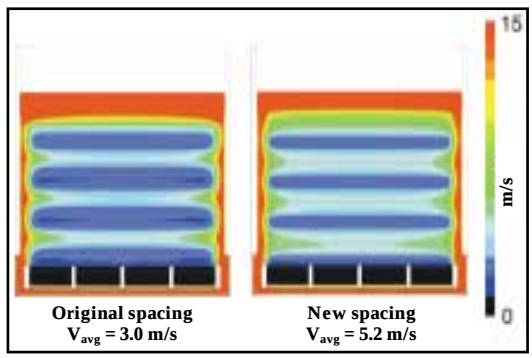

Fig. 12 — Comparison of flow through the load for original and new gear spacings.

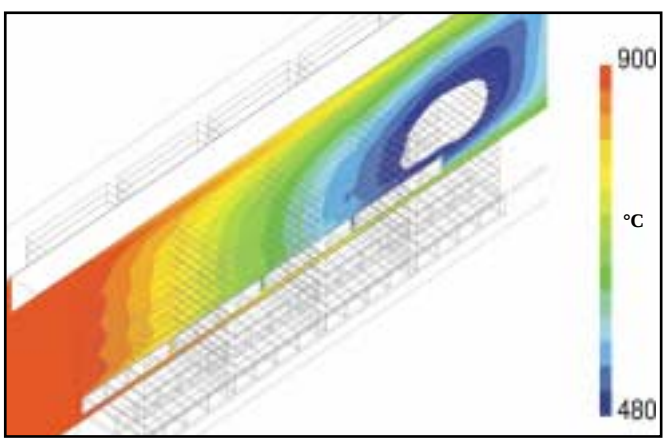

Fig. 13 — Gas temperature distribution along furnace centerline at 10 minutes into the heating cycle.

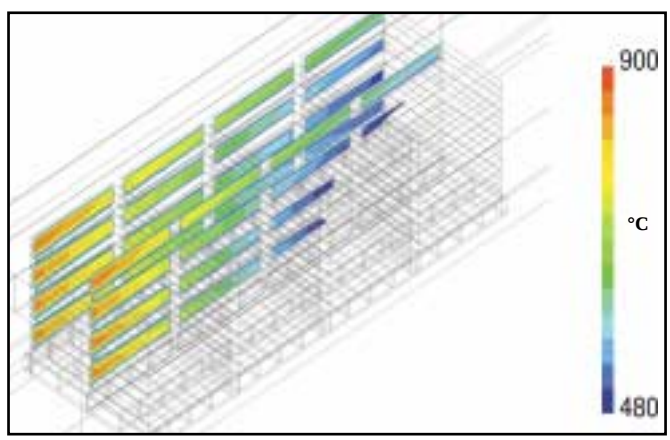

Fig. 14 — Gear temperature distribution along furnace centerline and edge of load at 10 minutes into the heating cycle.

seen in the flow direction due to the high thermal load of the parts. Higher temperatures are seen near the top of the load due to higher velocities and the contribution of radiation from the ceiling. The lowest temperatures are seen at the bottom portion of the fourth stack. The higher gas temperatures behind the load are due to recirculating flow in the open section downstream of the load.

Gear temperatures are presented in Fig. 14 for a centerline and side cut through the load at 10 minutes into the heating cycle. The gear temperature patterns closely follow the gas temperature patterns due to the large gear surface area exposed to the flow. This figure also shows a variation in temperature between the centerline of the load and the side, particularly toward the back of the load. This variation is largely due to the contribution of sidewall radiation.

The gear temperature history for 16 selected locations along the furnace centerline is presented in Fig. 15. Generally speaking, the gears heat up fastest toward the front of the load and slowest toward the rear. For the first stack, there is little vertical variation. The subsequent stacks show increasing vertical stratification, with the top fixture of gears in the fourth stack heating up faster than the bottom fixture in the third stack. Overall, the variation in gear temperatures is very small at the end of the two-hour heating cycle.

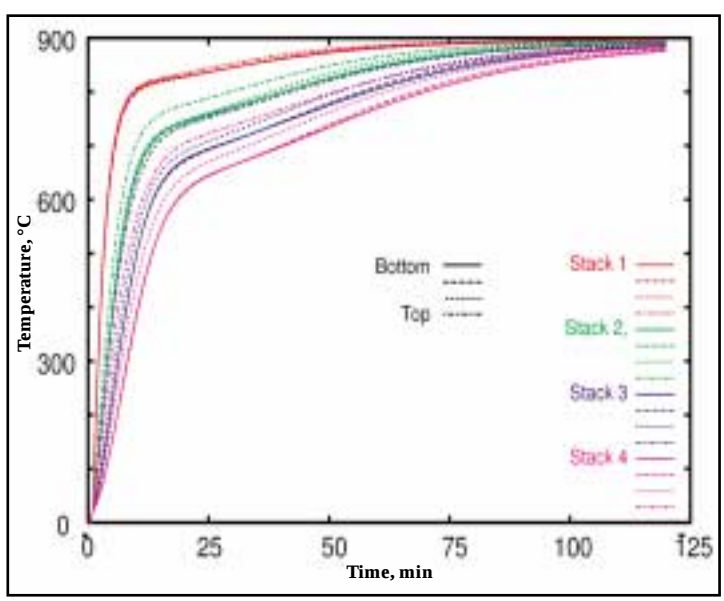

Fig. 15 — Temperature history of selected gears for the entire heating time.

Summary

The increasing use of gas flows in materials processing applications warrants further investigation into how the flow field affects surface heat transfer rates and the resultant product quality. To date, too little attention has been paid to these effects, relying instead on assumed surface heat transfer coefficients.